

Short Communication

Effects of Nickel and Silicon Content on the Corrosion Inhibition of Weathering Steels in Simulated Coastal Environments

Fenzhao Liu*

Department of Chemistry & Chemical Engineering, Lvliang University, Lvliang 033000, China

*E-mail: lfz31032@llhc.edu.cn

Received: 9 September 2020 / *Accepted:* 16 November 2020 / *Published:* 30 November 2020

The effect of Ni and Si elements on the corrosion behavior of weathering steels (WS) exposed to the simulated coastal environment was investigated by electrochemical measurement methods such as electrochemical impedance spectroscopy (EIS) and polarization technique. Morphology of specimens was studied using scanning electron microscopy and energy dispersive spectrometry. In polarization tests, with increasing Ni and Si content in WS, corrosion potential values shifted to more positive values and also the corrosion current density showed the lower values representing the higher corrosion protection. Fitting the EIS data to an appropriate equivalent electrical circuit demonstrated that the highest protection belonged to a WS0.5Si-0.5Ni sample that was consistent with polarization results. In fact, the density of the formed rust layer along with a good barrier function prevented remarkably the higher corrosion of the surface. It means that the passages of charge transfer were blocked and the dissolution reaction of metal surface carried out difficulty.

Keywords: Corrosion resistance; Electrochemical Impedance spectroscopy; Polarization; Weathering steel

1. INTRODUCTION

The corrosion resistance of weathering steels (WS) or low-alloy steels is higher in comparison with that of carbon steel. This property is attributed to the addition of some alloying elements such as Cu, Cr, Ni, P, Si, and Mn with a few percent maximum [1-3]. The corrosion inhibition of WS can be enhanced because of the formation of a protective dense layer with a good adhesion named the rust layer as a corrosion product. The rust layer has attractive appearance and self-healing properties. The alloying elements of steel and the environment affect the properties of the rust layer. Hence, to enhance the protection of the rust layer some alloying elements are added to steel containing less than

5 wt% [4, 5]. Weathering steels with higher mechanical strength and corrosion inhibition compared to mild steel and plain carbon steel are used in bridges, road installations, and facades and roofing [6].

It has reported that increasing the content of silicon in the steel was effective to increase the corrosion protection [7]. Si as an abundant element in nature can be used in the weathering steel because of the low cost and wide applications. Formation of martensite/austenite (M/A) constituents and as a result deteriorating the impact toughness of zones can be due to the adding a high amount of it [8, 9]. However, the tensile strength of WS with adding Si without increasing the content of carbon can be improved [10]. Kim et al. reported that Si via interaction with other elements can enhance the corrosion protection of WS [11]. Studies showed that the resistance of the formed rust layer can be improved by combination of Si and Al. These elements have a tendency to form nano-scale complex iron oxide in the iron rust layer which reduces the corrosion reactions [12-14]. Moreover, in a report J.A. Mejia Gomez et al. carried out an investigation about the addition of Si element in the low-alloy steel exposed to the marine environment. They realized that corrosion resistance of steel increased with increasing the Si content because of the formation of a rust layer containing fine grains [15]. Moreover, among the alloying elements, nickel indicates the best performance [16, 17]. Kimura et al. studied the steel with the high content of Ni in the coastal environment for a long time. They realized that Ni was distributed in both outer and inner layers (rust layers) especially with the higher content in the inner layer. Na^+ and also the Cl^- were distributed in the inner and outer layer, respectively. Therefore, the steel containing 3wt% Ni indicated a much lower ingress of ions compared to the WS. They considered for WS containing 3 wt% nickel with formation of Fe_2NiO_4 , a dense rust layer with fine grains is produced [18-20]. Also enhancement corrosion resistance of steel is achieved by adding Ni to the weathering steel in an atmosphere with high salinity. The effects of Ni and also the synergistic effects of nickel with other alloying elements on corrosion protection on weathering steel were studied. This property is related to formation of a rust layer on its surface with high protection [21, 22]. Due to the formation of Fe_2NiO_4 spinel double oxide and compact rust layer, steels containing nickel show good corrosion resistance [23, 24].

Since, the simultaneous effects of Ni and Si on corrosion resistance of weathering steel have not been previously reported. In this work the effects of adding different contents of Ni and Si elements to the weathering steel on the electrochemical corrosion protection of WS exposed to the simulated coastal environment were studied. The corrosion behavior of specimens was studied using EIS and polarization measurements. Also morphology and elemental analysis of WS materials were done using scanning electron microscopy and EDS analysis.

2. MATERIALS AND METHODS

The chemical compositions of four low-alloy steels named Ref, WS0.3Si-0.3Ni, WS0.4Si-0.4Ni and WS0.5Si-0.5Ni are described in Table 1. COR-TEN steel was used in this work. The specimens were cut to sizes 30 mm ×30 mm ×5 mm. All samples were ground with water sandpaper up to a grit size of 1000, and then degreasing, cleaning and rinsing in acetone with ultrasonic. After that the specimens dried at environment temperature.

Table 1. Chemical compositions of used materials.

Elements	C	Si	P	Mn	S	Cu	Ni	Cr	Ti	Fe
Ref	0.045	0.30	0.081	0.41	0.005	0.3	-	0.20	0.02	Bal.
WS0.3Si-0.3Ni	0.045	0.30	0.081	0.41	0.005	0.3	0.30	0.22	0.02	Bal.
WS0.4Si-0.4Ni	0.045	0.40	0.081	0.41	0.005	0.3	0.40	0.27	0.02	Bal.
WS0.5Si-0.5Ni	0.045	0.50	0.081	0.41	0.005	0.3	0.50	0.32	0.02	Bal.

The following steps for wet dry cyclic corrosion test were done: weighing the initial specimen, immersing the surface of sample with 0.05 M NaCl solution (simulated coastal environment based on the chloride concentration in the atmosphere of Wanning city, China [25]) for 12 min, drying the samples for 48 min at 25 °C and 60% RH (relative humidity). Therefore, each cycle was an hour. The specimens were taken out after 48, 96, 144 and 192 h, respectively. The corrosion products formed on the sample surfaces in a solution containing 50 ml distilled water, 50 ml hydrochloric acid and 0.35 g hexamethylenetetramine for almost 10 minutes. After removing the rust layers, they were rinsed with distilled water, dried with warm air, and after that for calculating the mass loss were weighed.

Electrochemical impedance spectroscopy (EIS) and polarization measurements were performed using a cell with three electrodes consisted of a saturated calomel reference electrode (SCE), a platinum counter electrode and steel sample as a working electrode with an exposed area of 1 cm². EIS was done over a frequency range from 100 kHz to 10 mHz by 10 mV sinusoidal potential modulations around to the open circuit potential. Also all samples before the EIS test were placed in the corrosive environment for stabilization for 60 minutes. The corrosive solution was 0.05 M NaCl solution. Polarization plots were obtained with a scan rate of 1 mV/s. In order to determine the corrosion current density and the corrosion potential values, Tafel extrapolation of polarization plots about 50-100 mV away from E_{corr} was carried out [26]. All the measurements were performed at room temperature. All electrochemical tests were done using an Ivium potentiostat and EIS data were analyzed using ZSimpWin software. The surface morphologies of specimens were obtained by Zeiss Sigma 300 VP scanning electron microscope.

3. RESULT AND DISCUSSION

3.1 Electrochemical Experiments

Figure 1 shows the open circuit potential (OCP) versus time for various WS materials in 0.05 M NaCl solution. It can be seen that the potential values shift to the positive direction for all WS samples which indicate the formation of protective rust layers. After about 60 minutes the potential values approach stable values.

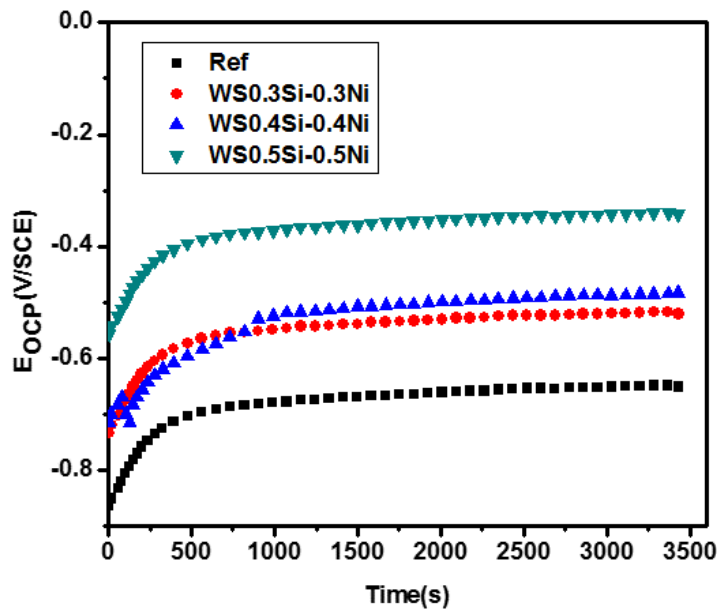


Figure 1. The open circuit potential versus time curves of different WS materials in 0.05 M NaCl solution.

Electrochemical impedance spectroscopy (EIS) measurements were done to investigate the corrosion behavior of different Ni and Si contents of weathering steel. Figure 2 (a,b) shows the Nyquist and bode diagrams of the WS samples in 0.05 M NaCl solution before the wet-dry process.

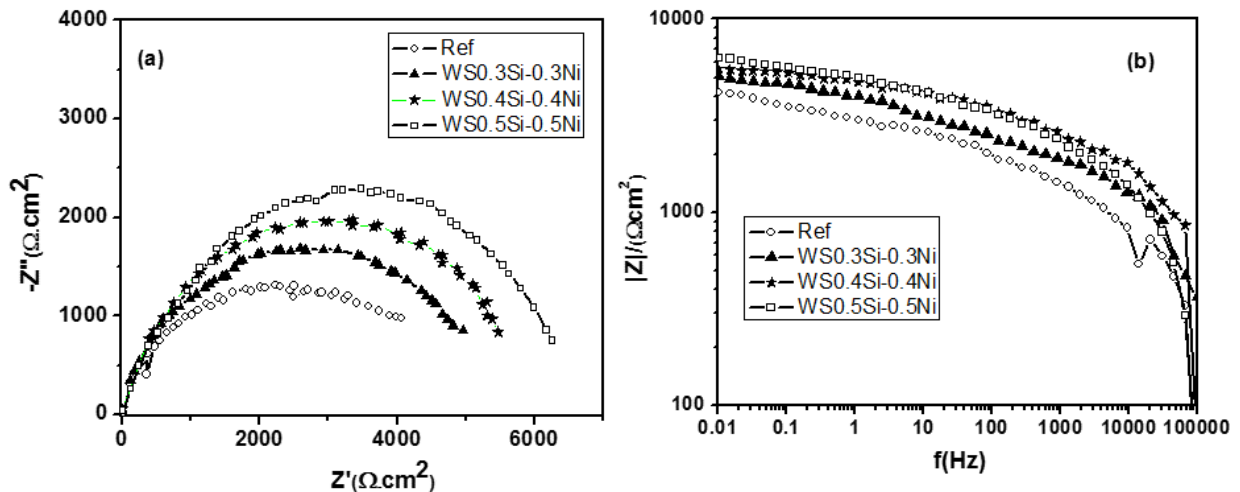


Figure 2. a) Nyquist and b) Bode plots for different WS materials exposed to the 0.05 M NaCl solution before the wet-dry cyclic test

Figure 3 presents the electrical equivalent circuit applied for fitting the EIS results. Nyquist diagrams reveal two capacitance loops, one loop is related to the formation of a small amount of initial corrosion products on specimen surfaces and the other one in high frequency is related to the charge transfer resistance at the interface between the sample and the solution. In the electrical equivalent circuit, R_s is the solution resistance. R_{film} is the resistance of corrosion products which is attributed to

the density and the thickness of the rust layer. R_{ct} is the charge transfer resistance. Also CPE_{film} and CPE_{dl} which are used to replace the pure capacitance element to explain the capacitance behavior [27, 28]. These constant phase elements (CPE) exhibit electrochemical behaviors of the layers containing corrosion products and the double layer capacitance, respectively.

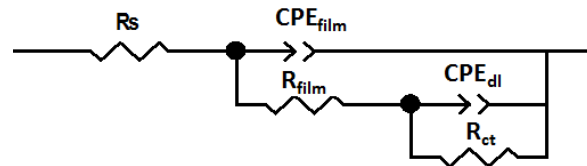


Figure 3. The used equivalent circuit in EIS test

As shown in Table 2 from the fitted EIS results, R_{ct} values increase with the increasing the content of Ni and Si in WS materials. It means that the passages of charge transfer are blocked. Therefore, the dissolution reaction of the metal surface carries out difficulty. Moreover, increasing the values of R_{film} exhibits that the addition of alloying elements to weathering steels improves the formed rust layers with higher coverage [29, 30]. Obtained resistances values for WS0.5Si-0.5Ni sample are significantly higher than ones for other samples. It can be concluded that the highest Si and Ni content in WS enhances the density of the rust layer along with a good barrier function which can remarkably prevent the higher corrosion of the surface [31].

Table 2. Parameter values obtained from the fitting the EIS results for WS samples

Materials	$R_s(\Omega)$	$R_f(\Omega \text{ cm}^{-2})$	$CPE_f(\Omega^{-1} \text{ cm}^{-2} \text{ s}^n)$	n_f	$R_{ct}(\Omega \text{ cm}^{-2})$	$CPE_{dl}(\Omega^{-1} \text{ cm}^{-2} \text{ s}^n)$	n_{dl}
Ref	19	1100	1.47×10^{-4}	0.76	3000	5.12×10^{-4}	0.47
WS0.3Si-0.3Ni	20	1485	1.36×10^{-4}	0.78	3528	4.12×10^{-4}	0.52
WS0.4Si-0.4Ni	18	1904	1.05×10^{-4}	0.81	3913	2.13×10^{-4}	0.65
WS0.5Si-0.5Ni	19	2334	9.1×10^{-5}	0.83	4164	1.01×10^{-4}	0.71

Figure 4 shows the polarization measurement for various contents of Ni and Si in weathering steel materials in the simulated coastal environment. The obtained values from polarization curves such as corrosion potential, corrosion current density and Tafel slopes are presented in Table 3. As we can see in Figure 4 the polarization curves indicate the similar behavior so that both Tafel slopes have almost similar values. It can be considered that various content of Si and Ni in the weathering steel cannot significantly affect the reaction of the electrode [31-33]. The increasing the corrosion potential and reducing the current density values of samples with use of Ni and Si elements in weathering steel confirms that these alloying elements can enhance the corrosion inhibition of samples [34, 35].

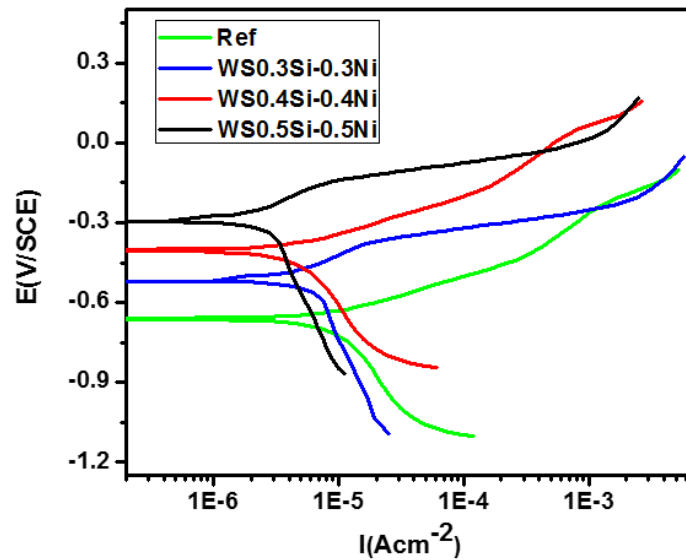


Figure 4. Polarization curves of WS materials in 0.05 M NaCl before the wet-dry cyclic test

Studies have indicated that the oxides produced by Si (silicon oxides) are fine which can refine the corrosion products by entering the crystal gaps. These complex oxides in the rust layer have effects on the densification and the electrochemical behavior of the corrosion products [7, 36]. Moreover, precipitating the Si alloying element in WS from the steel matrix may influence the anodic corrosion reaction. Presence of Si element retards the mass transfer with creating the rust layer with the higher stability and compactness. The addition of Ni can improve both of the corrosion resistance and the mechanical properties of the steel. Generally, Ni exists in NiO and NiFe₂O₄ spinel in the rust layer. The NiO can increase the stability of the rust layer by promoting the crystallization of corrosion products. Increasing the amount of Ni leads to an increase in the number of NiO particles and appearing NiFe₂O₄ particles. These stable Ni oxides with the thickness of the rust layer to inhibit the higher corrosion of the steel [37].

Table 3. Obtained corrosion parameters from polarization curves

Materials	E_{Corr} (V) vs. SCE	i_{Corr} ($\mu\text{A}/\text{cm}^2$)	β_a (mV/dec)	$-\beta_c$ (mV/dec)
Ref	-0.664	5.12	80	297
WS0.3Si-0.3Ni	-0.523	4.03	76	305
WS0.4Si-0.4Ni	-0.406	2.53	74	300
WS0.5Si-0.5Ni	-0.301	1.78	71	307

3.2. Corrosion rate

The corrosion rate of different weathering steel materials after the corrosion tests can be obtained using the equation $\frac{m}{\rho_{st}}$, where m is the mass loss, ρ is the density, t is the corrosion test time and s is the surface area of specimens. Figure 5 exhibits the corrosion rate of different WS materials containing Ni and Si in the simulated coastal environment. A similar trend with the quick decline at the

initial stage is observed for the corrosion rates of different kinds of weathering steels. It can be considered that the protective rust layer has not completely formed and the corrosion rate of the WS samples pursues a similar corrosion rule. In fact, corrosion inhibition of different kinds of weathering steels is enhanced with increasing the amount of Ni and Si at every corrosion cycle and Ref and WS0.5-Si0.5Ni samples show the highest and lowest corrosion rate, respectively. It means that the corrosion products formed on the sample surfaces show a barrier property to the diffusion of oxygen and penetration of chloride ions which results in the enhancement of the corrosion protection. These results are consistent with the obtained EIS and polarization results.

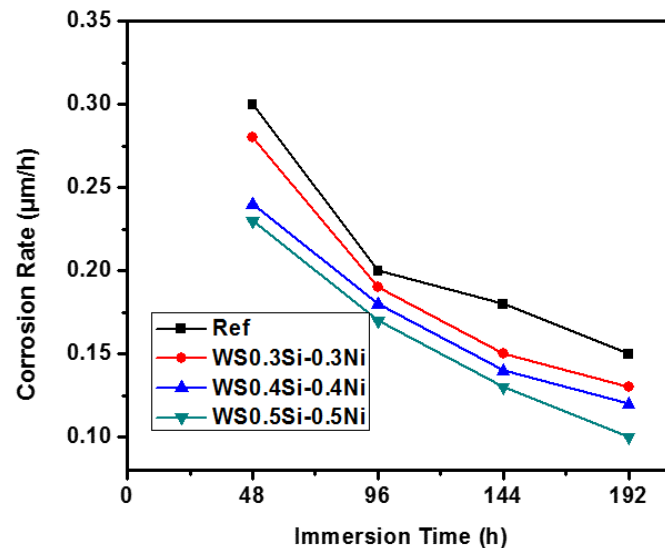


Figure 5. Corrosion rate of different weathering steel materials as a function of immersion time

3.3 Micromorphology of the rust layer

There is a connection between the corrosion inhibition of weathering steel and the nature of formed rust layers on the sample. Figure 6 shows the micromorphology of the rust layer on Ref and WS0.5Si-0.5Ni samples at the 192 h (Cycles), respectively. The rust layers formed on weathering steels become smoother and less porous with increasing the Si and Ni contents in WS. The less porous structure of the formed rust layer results in lower corrosion rate because of the more effective barrier against the penetration of chloride ions and precipitation. The rust layer is composed of the adherent and compact inner layer with a higher effective corrosion inhibition and also a less adherent and porous outer layer [2]. The thickness of rust layers increases with time along with the denser and uniform inner layer which can protect samples from the higher corrosion. The adhesion and compactness of rust layers become higher with increasing Si and Ni content in WS.

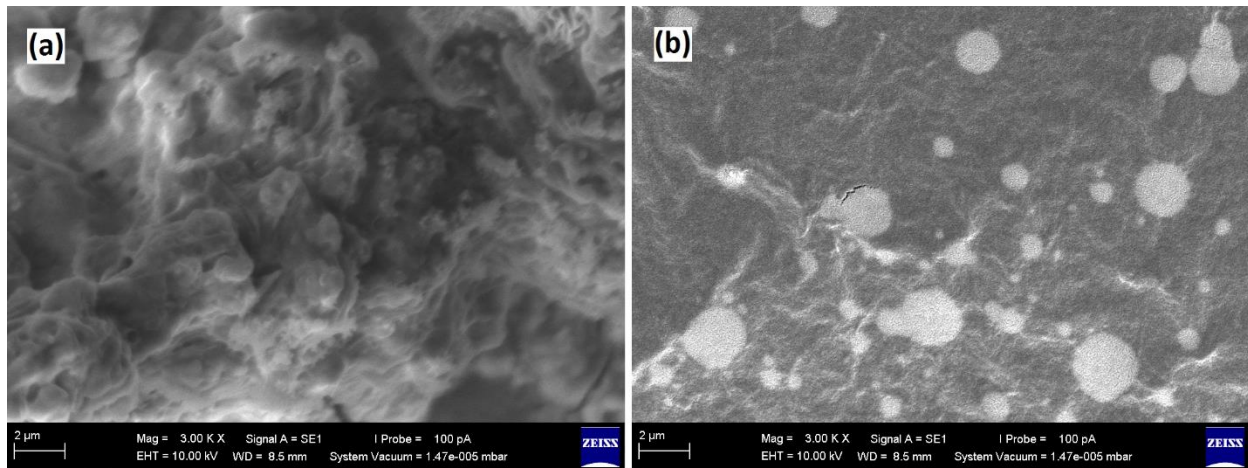


Figure 6. SEM micromorphology of a) Ref and b) WS0.5Si-0.5Ni at 192 h, respectively

EDS elemental analysis was carried out on the rust layers to qualitatively determine the presence of alloying elements especially adding ones such as Si and Ni. Result of EDS for WS0.5Si-0.5Ni sample at 192 h of corrosion process is given in Figure 7. Table 4 shows the distribution of Ni and Si elements in the outer and inner rust layer after 192 h of corrosion process. It should be considered that the deposition amount of chloride ions can affect the corrosion rate [38]. As shown in Table 4, the presence of Ni and Si is observed higher in the inner rust layer. In addition, it is observed that for Ref sample Na^+ and Cl^- content are higher in the outer layer and inner layer, respectively. For this sample, ingress of Cl^- is easier for the rust layer to corrode the metal and Na^+ hydrolysis leads to decreasing pH value which increases the anodic dissolution of metal surface.

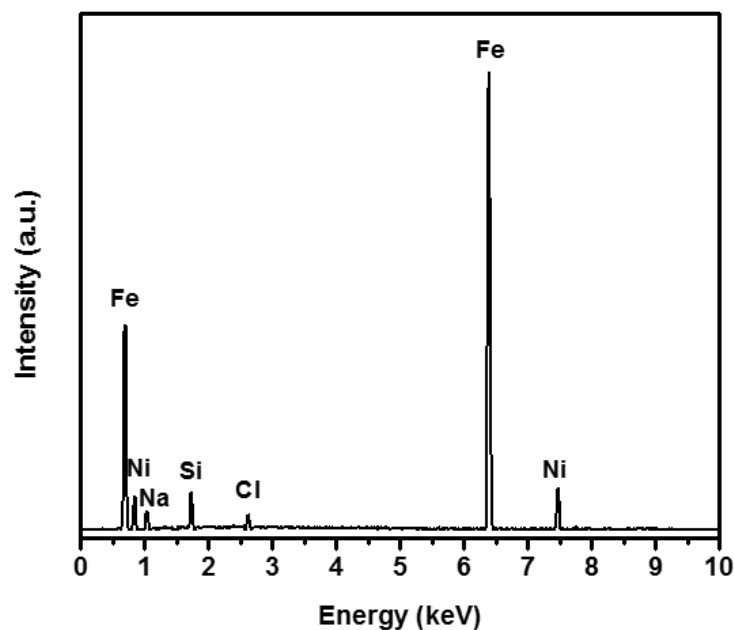


Figure 7. EDS for WS0.5Si-0.5Ni sample at 192 h of corrosion process.

Table 4. Weight percent of Si and Ni elements in the rust layer

Materials	Rust layer	Ni	Si
Ref	Outer	-	0.11
	Inner	-	0.16
WS0.3Si- 0.3Ni	Outer	0.23	0.18
	Inner	0.29	0.24
WS0.4Si- 0.4Ni	Outer	0.35	0.31
	Inner	0.38	0.37
WS0.5Si- 0.5Ni	Outer	0.39	0.41
	Inner	0.47	0.43

4. CONCLUSION

The corrosion behavior of weathering steels containing different Ni and Si contents in the simulated coastal environment was studied by electrochemical methods such as EIS and polarization technique. Morphology of specimens was studied using SEM and EDS. The rust layers produced on weathering steels became smoother and less porous with increasing the Si and Ni contents. The less porous structure of the rust layer led to the lower corrosion rate because of the more effective barrier against the penetration of chloride ions and precipitation. In polarization tests, with increasing Ni and Si content in WS corrosion potential values shifted to more positive values and also the corrosion current density showed the lower values representing the higher corrosion protection. Fitting the EIS data to an appropriate equivalent electrical circuit demonstrated that the highest protection belonged to a WS0.5Si-0.5Ni sample that was consistent with polarization results.

ACKNOWLEDGEMENT

This work was supported by Scientific and Technological Innovation Programs of Higher Education Institutions in Shanxi (2019L0968); Construction Plan of Key Disciplines of “1331 Project” in Shanxi Province (Materials Science and Engineering); Construction Project of Superiority and Characteristic Specialty in Shanxi Colleges and Universities (Materials Chemistry).

References

1. X. Chen, J. Dong, E. Han and W. Ke, *Materials Letters*, 61 (2007) 4050.
2. Q. Zhang, J. Wu, J. Wang, W. Zheng, J. Chen and A. Li, *Materials Chemistry and Physics*, 77 (2003) 603.
3. S. Kakooei, H.M. Akil, M. Jamshidi and J. Rouhi, *Construction and Building Materials*, 27 (2012) 73.
4. H. Townsend, *Corrosion*, 57 (2001) 497.
5. J. Rouhi, S. Mahmud, S.D. Hutagalung and S. Kakooei, *Journal of Micro/Nanolithography, MEMS, and MOEMS*, 10 (2011) 043002.
6. S. Kakooei, H.M. Akil, A. Dolati and J. Rouhi, *Construction and Building Materials*, 35 (2012) 564.

7. S.J. Oh, D. Cook and H. Townsend, *Corrosion Science*, 41 (1999) 1687.
8. G. Laird and G.L. Powell, *Metallurgical Transactions A*, 24 (1993) 981.
9. J. Yang, Y. Lu, Z. Guo, J. Gu and C. Gu, *Corrosion Science*, 130 (2018) 64.
10. W. Garrison, *Metallurgical Transactions A*, 17 (1986) 669.
11. K. Kim, Y. Hwang and J. Yoo, *Corrosion*, 58 (2002) 570.
12. T. Nishimura, *Corrosion science*, 52 (2010) 3609.
13. T. Nishimura, *Corrosion Science*, 50 (2008) 1306.
14. J. Rouhi, S. Mahmud, S. Hutagalung and S. Kakooei, *Micro & Nano Letters*, 7 (2012) 325.
15. J.M. Gómez, J. Antonissen, C. Palacio and E. De Grave, *Corrosion science*, 59 (2012) 198.
16. G. Cao and W. CHANG, *Acta Metall Sin*, 46 (2010) 748.
17. H. Naitô, Y. Hosoi, H. Okada and K. Inouye, *Corrosion Engineering Digest*, 16 (1967) 191.
18. C. Wen, Y. Tian, G. Wang, J. Hu and P. Deng, *International Journal of Electrochemical Science*, 11 (2016) 4161.
19. M. Kimura, T. Suzuki, G. Shigesato, H. Kihira and K. Tanabe, *Nippon Steel Tech. Rep.*, 87 (2003) 17.
20. M. Kimura, H. Kihira, N. Ohta, M. Hashimoto and T. Senuma, *Corrosion Science*, 47 (2005)
21. J. Castaño, C. Botero, A. Restrepo, E. Agudelo, E. Correa and F. Echeverría, *Corrosion Science*, 52 (2010) 216.
22. D. Singh, S. Yadav and J.K. Saha, *Corrosion Science*, 50 (2008) 93.
23. T. Nishimura and T. Kodama, *Corrosion Science*, 45 (2003) 1073.
24. T. Nishimura, H. Katayama, K. Noda and T. Kodama, *Corrosion Science*, 42 (2000) 1611.
25. L. Hao, S. Zhang, J. Dong and W. Ke, *Corrosion Science*, 58 (2012) 175.
26. H.S. Bahari and H. Savaloni, *EPL (Europhysics Letters)*, 129 (2020) 18003.
27. H.S. Bahari and H. Savaloni, *Metals and Materials International*, (2019) 1.
28. J. Rouhi, S. Kakooei, M.C. Ismail, R. Karimzadeh and M.R. Mahmood, *International Journal of Electrochemical Science*, 12 (2017) 9933.
29. Z. Malaibari, R. Kahraman, H. Saricimen and A. Quddus, *Corrosion engineering, science and technology*, 42 (2007) 112.
30. Z. Feng, X. Cheng, C. Dong, L. Xu and X. Li, *Corrosion Science*, 52 (2010) 3646.
31. R. Sun, Q. Yu, Y. Zhang, X. Yan, Y. Lu, C. Zhang and Q. Wang, *Metals*, 9 (2019) 486.
32. W. Wu, X. Cheng, H. Hou, B. Liu and X. Li, *Applied Surface Science*, 436 (2018) 80.
33. Y. Fan, W. Liu, Z. Sun, T. Chowwanonthapunya, Y. Zhao, B. Dong, T. Zhang, W. Banthukul and X. Li, *Journal of Materials Engineering and Performance*, 12 (2020) 1.
34. I. Díaz, H. Cano, P. Lopesino, D. De la Fuente, B. Chico, J.A. Jiménez, S.F. Medina and M. Morcillo, *Corrosion Science*, 141 (2018) 146.
35. T. Zhang, W. Liu, Z. Yin, B. Dong, Y. Zhao, Y. Fan, J. Wu, Z. Zhang and X. Li, *Journal of Materials Engineering and Performance*, 29 (2020) 1.
36. M. Murayama, T. Nishimura and K. Tsuzaki, *Corrosion science*, 50 (2008) 2159.
37. D.-l. Li, G.-q. Fu, M.-y. Zhu, Q. Li and C.-x. Yin, *International Journal of Minerals, Metallurgy, and Materials*, 25 (2018) 325.
38. T. Kamimura, K. Kashima, K. Sugae, H. Miyuki and T. Kudo, *Corrosion science*, 62 (2012) 34.